Asian Journal of Chemistry; Vol. 32, No. 12 (2020), 3097-3104

ASIAN JOURNAL OF CHEMISTRY

https://doi.org/10.14233/ajchem.2020.22897

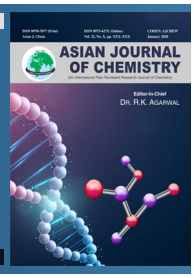

Electrochemical and Theoretical Studies of 2-Acetyl Pyridine and Acetophenone Derivatives as Corrosion Inhibitors for Mild Steel in HCl Solution

DHARMENDRA KUMAR SINGH[1,*] and MANTU KR. SINGH[2]

[1]Department of Chemistry, B.B.M.K. University, Dhanbad-828130, India
[2]Department of Chemistry, Raja Shiv Prasad College, Jharia-828111, India

*Corresponding author: E-mail: dksslnt@gmail.com

Received: 13 July 2020; *Accepted*: 25 September 2020; *Published online*: 7 December 2020; AJC-20146

2-Acetyl pyridine nicotinic hydrazone and acetophenone nicotinic hydrazone have prepared and their corrosion inhibition properties for mild steel in 1 M HCl were studied using weight loss, electrochemical and density functional theory (DFT) methods. Both inhibitors showed good inhibition ability and their adsorption on mild obeyed Langmuir adsorption isotherm. Polarization measurements show that they can be classified as inhibitors of mixed type. The inhibition efficiencies of 2-acetyl pyridine nicotinic hydrazone and acetophenone nicotinic hydrazone at 2 mM optimum concentration are 96.5% and 87.7% respectively.

Keywords: 2-Acetyl pyridine nicotinic hydrazone, Acetophenone nicotinic hydrazone, Mild steel, Acid corrosion, Adsorption.

INTRODUCTION

Among various metals, mild steel is a widely used structural material due to its mechanical strength, availability and cost effectiveness, but its susceptibility towards corrosion particularly in acidic media is a matter of concern among researchers and academicians since long time. As the use of hydrochloric acid is very efficient, easy in handling, cheaper and easily available, hence it is commonly used in the acid pickling, acid cleaning, oil well cleaning, petrochemical industry, *etc.* [1,2]. This leads to centre of attention on the protection of mild steel under acidic environment especially in hydrochloric acid media. There are various methods to protect metal under acidic conditions but the use of inhibitors is one of the most practical and efficient method. It has been reported that organic compounds containing nitrogen, sulphur, oxygen, π-electrons as well as aromatic ring in their structure are very effective in protection of mild steel from corrosion in acidic media. These inhibitors block the active sites on the metal surface by adsorption process either by chemisorption or physisorption mechanism and prevent the attack of metal surface by acidic solution [3-8].

Literature survey also reveals that the Schiff bases have widely been investigated organic compounds as corrosion inhibitors for mild steel in HCl solution. These compounds show good inhibition efficiency due to presence of –CH=N– group in their structure which make it capable to coordinate with mild steel in acid solution. Due to cheaper raw materials requirement, ease in preparation and handling again make Schiff bases very popular among researchers [9,10].

Nicotinic hydrazones are non-toxic and have various pharmacological properties like anti-inflammatory, analgesic and antimicrobial activities [11]. We have already reported 4-(*N*,*N*-dimethylamino)benzaldehyde nicotinic hydrazine (ABNH), *N*′-(4-Hydroxybezylidene)nicotinic hydrazone (HBNH) and *N*′-(4-methylybezylidene)nicotinic hydrazone (MBNH) as corrosion inhibitors for mild steel in 1 M HCl, where they have shown high inhibition efficiency at 30 ºC [12,13]. Keeping this in view, the objective of this study was to evaluate the corrosion inhibition ability of two synthesized hydrazones namely 2-acetyl pyridine nicotinic hydrazone (2-APN) and acetophenone nicotinic hydrazone (ACN) for mild steel in 1 M HCl using potentiodynamic polarization and electro-chemical impedance spectroscopy. The effect of temperature on the corrosion behaviour of mild steel in 1 M HCl with opti-mum concentration of inhibitor was also studied in the temperature range 303-323 K. To correlate molecular parameters with

inhibition ability of the inhibitors various molecular parameters like energy of highest occupied molecular orbital (E_{HOMO}), energy of lowest unoccupied molecular orbital (E_{LUMO}), energy gap ($\Delta E = E_{LUMO} - E_{HOMO}$) and dipole moment ($\mu$) of the inhibitor molecules were calculated using density functional theory (DFT).

EXPERIMENTAL

Synthesis of nicotinic hydrazone: Nicotnic hydrazones were synthesized by mixing equimolar quantity of nicotinic acid hydrazide dissolved in ethanol with 2-acetyl pyridine or acetophenone. On refluxing reactants mixture for 4 h on oil bath followed by cooling, the precipitate was obtained [11]. The products were recrystallized in ethanol. The purity and the structure of the hydrazones were checked by TLC, IR and ^{1}H NMR techniques.

The corrosion tests were performed on the mild steel having chemical composition (wt %): C: 0.07, Mn: 0.42, P: 0.029, S: 0.014, Al: 0.041 and rest Fe. The mild steel as working electrode was embedded in epoxy resin in such a way that only cross sectional area of 1 cm^2 could make contact with test solution. Prior to each experiment, the exposed mild steel surface was abraded with emery papers (grade 320 to 1200), washed with double distilled water and dried with cool air. The test solution 1M HCl was prepared by dilution of analytical grade 37% HCl solution with double distilled water. The concentration of the corrosion inhibitors was kept in the range of 0.01 to 2.00 mM.

Electrochemical measurements: Prior to each electrochemical test, the working electrode was immersed in the test solution and left to attain steady-state open circuit potential (OCP). The electrochemical impedance measurements were carried out at the steady state over a frequency range of 100 kHz-0.1 Hz with 5 mV peak-to-peak amplitude using the AC signal.

The potentiodynamic polarization measurements were carried out in the potential range -250 to +250 mV relative to the OCP at a scan rate of 1 mV s^{-1}. Platinum rod was used as counter electrode, saturated calomel electrode (SCE) as the reference electrode and the working electrode mild steel. Measurements were carried out using CHI 660C Electrochemical Workstation. All the electrochemical analysis were performed at 30 ºC in a three electrode assembly in stagnant condition.

The percentage inhibition efficiency (η %) was calculated using the following equation as [13]:

$$\eta\ (\%) = \frac{i^{o}_{corr} - i_{corr}}{i^{o}_{corr}} \times 100 \quad (1)$$

where i^{o}_{corr} and i_{corr} are corrosion current density values in the absence and presence of inhibitors, respectively [14].

$$\eta\ (\%) = \frac{R_p - R^{o}_{p}}{R_p} \times 100 \quad (2)$$

where R_p and R^{o}_{p} are the polarization resistance in the presence and absence (blank solution) of inhibitor, respectively.

Weight loss measurements: To explore thermodynamic kinetic parameters for the corrosion of mild steel in 1 M HCl, mild steel specimens in triplicate were immersed in 1 M HCl in the presence and absence of the optimum concentration of 2 mM of the inhibitors (2-APN and ACN) for 3 h at the different temperature ranging from 30-50 ºC. The mass of each mild steel specimen was determined before and after immersion and the average of the triplicate measurements was used to calculate corrosion rate. The corrosion rate (C_R) was calculated as follows:

$$C_R = \frac{\Delta w}{S \times t} \quad (3)$$

where Δw is the weight loss after corrosion, S is the total surface area of the mild steel specimen, 't' is time of exposure.

Quantum chemical calculation: Quantum chemical calculations were performed with complete geometry optimization using density functional theory (DFT) method at B3LYP/6-31++ G (d,p) level as implemented in Gaussian 09W (interfaced with Gauss View 5.0 as molecular modeller) software. The important molecular parameters like E_{HOMO}, E_{LUMO}, energy gap (ΔE) and dipole moment (μ) for the neutral and the protonated inhibitor molecules were calculated.

Adsorption isotherm and thermodynamic parameters: The study of adsorption isotherm can be used to understand the adsorption mechanism of the inhibitors on mild steel surface and their inhibition ability to protect from the corrosion. The various isotherms like Freundlich, Temkin and Langmuir are tested using potentiodynamic polarization measurements at 30 ºC.

RESULTS AND DISCUSSION

FT-IR spectra: FT-IR spectra of 2-acetyl pyridine nicotinic hydrazone (2-APN) and acetophenone nicotinic hydrazone (ACN) showed the following absorption bands: **2-APN** (KBr, ν_{max}, cm^{-1}): 3430, 3321, 3215, 3092, 1661, 1585, 1291, 1150, 976, 710; **ACN** (KBr, ν_{max}, cm^{-1}): 3441, 3306, 3192, 3084, 1658, 1590, 1290, 1143, 978, 820, 696. The presence of -C=N- group (Schiff base) in the synthesized inhibitors have confirmed by the spectral peaks at 1585 cm^{-1} (2-APN) and 1590 cm^{-1} (ACN) in FT-IR spectra.

^{1}H NMR spectra: 2-APN: ^{1}H NMR (δ ppm, DMSO-d_6): 2.51 (s, 3H, -CH_3), 7.12-9.06 (8H, Ar-H), 11.07 (s, 1H, -NH-C=O). **ACN:** ^{1}H NMR (δ ppm, DMSO); 2.51(s, 3 H, -CH_3), 7.35-9.10 (9H, Ar-H), 11.00 (s, 1H, -NH-C=O). The data of ^{1}H NMR spectra confirmed the expected hydrogen distribution in the synthesized 2-APN and ACN.

Potentiodynamic polarization measurements: The potentiodynamic polarization curves of mild steel in 1 M HCl in the absence and presence of various concentrations of 2-APN and ACN are shown in Fig. 1. It can be seen that both anodic and cathodic tafel curves appreciably shift towards lower current density on addition of inhibitor to acidic solution and the magnitude of shifting increasing with increases in inhibitor concentration. It indicates that both the inhibitors retard the anodic and cathodic reactions. In current-potential curves, the cathodic part of the curves are almost parallel in the presence and absence of the inhibitors (Fig. 1); it suggests that the addition of inhibitors do not modify the mechanism of hydrogen

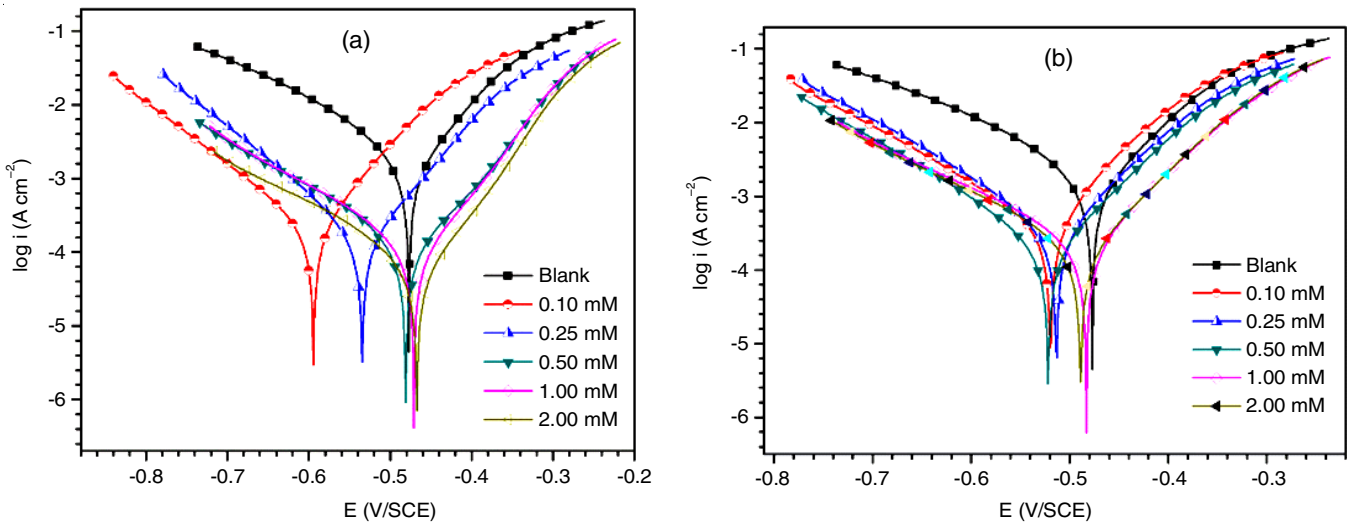

Fig. 1. Polarization curves for mild steel in 1 M HCl in the absence and presence of inhibitors: (a) 2-APN and (b) ACN

evolution or cathodic reaction mechanism, while they only modify kinetics of corrosion process.

The kinetics parameters like corrosion potential (E_{corr}), cathodic and anodic Tafel slopes (β_c and β_a) and corrosion current density (i_{corr}) obtained from the Tafel extrapolation of the polarization curves are given in Table-1. It is clear that there is no definite trend in the shifting of E_{corr} in the presence of inhibitor with respect to blank solution. It indicates that both 2-APN and ACN act as mixed type corrosion inhibitors. Further, the data in Table-1 also reveals that on increasing inhibitor concentration, there is significant decrease in corrosion current density. This may be owing to adsorption of inhibitor molecules on the mild steel surface that block the active sites on the metal surface. The inhibition efficiency of the inhibitors follow the order of 2-APN > ACN. The order of inhibition efficiency indicates that the presence of two pyridine ring in 2-APN makes it more capable to adsorb on mild steel surface than that of ACN, which only contain one such ring. The maximum efficiency values for 2-APN and ACN at 2 mM concentration are 96.5% and 87.7%, respectively.

Electrochemical impedance spectroscopy (EIS): The Nyquist plots of mild steel in1 M HCl in the absence and presence of 2-APN and ACN are given in Fig. 2. From these plots, it is apparent that each impedance spectra is a single slightly depressed semi-circle. It shows a non-ideal capacitive behaviour of the electrochemical solid/liquid interface [15,16]. It may be due to the surface roughness or the chemical inhomogeneities [17-19]. The diameter of the capacitive loops increases sharply with increasing inhibitor concentration. It can be related to increase of surface coverage of inhibitive molecules on metal surface [20,21]. The corresponding Bode plots for mild steel in 1 M HCl in the absence and presence of different concentration of inhibitors are shown in Fig. 3. In these Bode plots, one time constant is observed at all concentration of inhibitors. At lower frequency, the value of impedance is higher in the presence of inhibitor as compared to that in uninhibited solution. Furthermore, the impedance value significantly increases with increase in inhibitor concentrations. It indicates that these inhibitors have capability to protect mild steel in acidic solution. At a given concentration of inhibitor the impedance value in the presence of 2-APN is higher than that in ACN. It indicates that 2-APN has more inhibiting ability than ACN.

The impedance spectra were analyzed by fitting the experimental data to the equivalent circuit models as given in Fig. 4. To take into account heterogeneity of the electrode surface, impurities, adsorption of inhibitor molecules and dislocation, CPE is used in the equivalent circuits in place of double layer capacitance (C_{dl}) to give a more accurate fit to the experimental

TABLE-1
ELECTROCHEMICAL POLARIZATION PARAMETERS FOR MILD STEEL IN 1 M HCl SOLUTION IN THE ABSENCE AND PRESENCE OF 2-APN AND ACN AT 30 °C

Inhibitors	Conc. (mM)	$-E_{corr}$ (mV/SCE)	$-\beta_c$ (mV dec^{-1})	β_a (mV dec^{-1})	i_{corr} (mA cm^{-2})	η %
Blank		470	140.5	85.2	1.532	–
2-APN	0.10	593	115.6	81.0	0.210	86.3
	0.25	526	135.6	76.2	0.144	90.6
	0.50	464	149.3	79.1	0.110	92.8
	1.00	456	146.5	70.5	0.095	93.8
	2.00	452	144.8	65.4	0.053	96.5
ACN	0.10	528	122.7	82.5	0.431	71.8
	0.25	511	114.8	81.6	0.331	78.3
	0.50	478	149.3	78.6	0.219	85.6
	1.00	515	115.2	76.6	0.194	87.3
	2.00	480	145.3	75.7	0.188	87.7

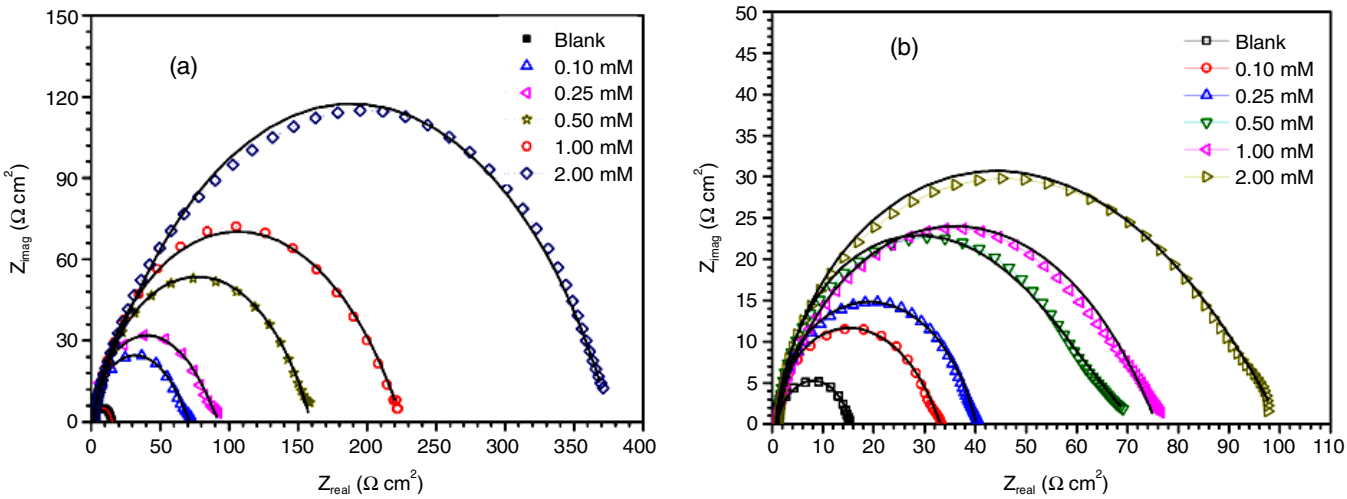

Fig. 2. Nyquist plots of mild steel in 1 M HCl in the absence and presence of various concentrations of the inhibitors: (a) 2-APN and (b) ACN (Solid lines represent fitted result)

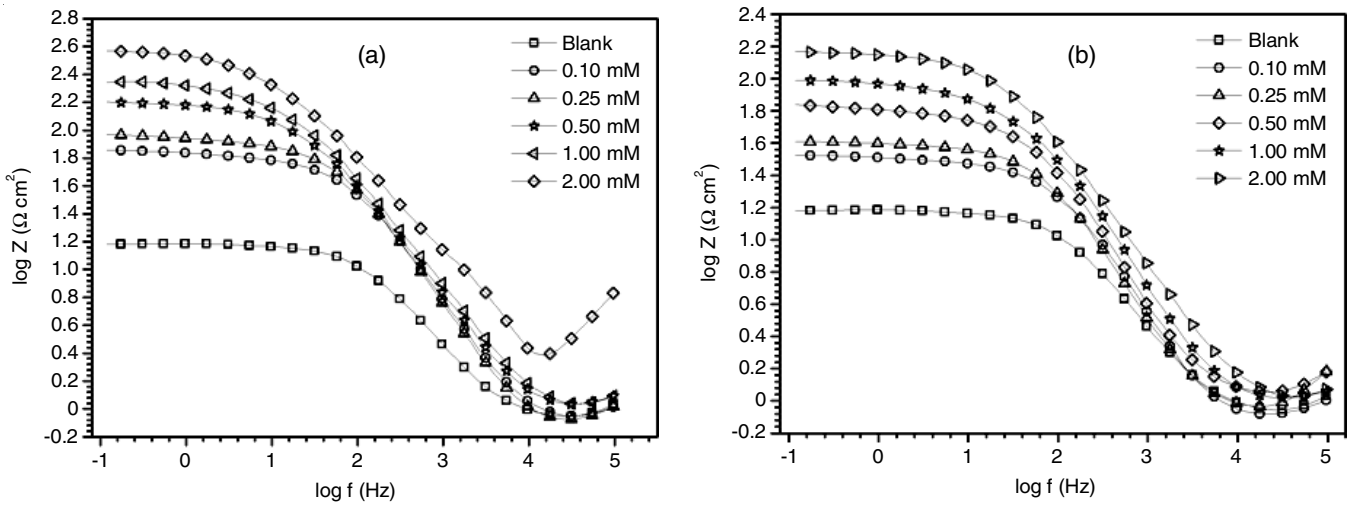

Fig. 3. Bode plots of mild steel in 1 M HCl in the absence and presence of various concentrations of the inhibitors: (a) 2-APN and (b) ACN

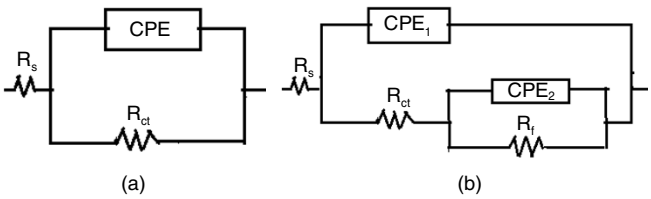

Fig. 4. Equivalent circuit diagrams: (a) In the absence of inhibitor, (b) In the presence of inhibitors

EIS data. The equivalent circuit models as shown in Fig. 4a and 4b fit well with the experimental data obtained in the absence and presence of inhibitors respectively as evident from Figs. 2 and 3. In Nyquist plots, the difference in real impedance at lower and higher frequencies is commonly considered as charge transfer resistance (R_{ct}); while in the present study, this difference is considered as the polarization resistance (R_p) as an alternative of charge transfer (R_{ct}). In the absence of inhibitor molecules, polarization resistance consist of only charge transfer resistance (R_{ct}), while in the presence of inhibitor, it is to the sum of R_{ct} and R_f [22]. R_f is the film resistance which correspond to adsorption of inhibitor molecules and/or all other accumulated kinds like corrosion product, inhibitor molecules, *etc*. at metal/solution interface [23,24].

The CPE impedance is composed of a component Y_0 and a coefficient n, which can be represented as follows [25,26]:

$$Z_{CPE} = Y_0^{-1}(j\omega)^{-n} \quad (4)$$

where Y_0 is a proportional factor; ω is angular frequency, j is imaginary number ($j^2 = -1$), n is a deviation parameter or phase shift ($-1 \le n \le +1$), which can be used as a gauge of the heterogeneity or roughness of the metal surface. The impedance parameters obtained by fitting EIS data to the equivalent circuits are shown in Table-2. It is evident that the values of R_p increases with the addition of inhibitor to acid solution; further this increase is more pronounced with increase in concentration of inhibitors. It can be attributed to the formation of protective layer at metal/solution interface and this layer acts as barrier for the mass and charge transfers. Conversely, the CPE values decrease with increase in inhibitors concentration which can be attributed to decrease in local dielectric constant and/or

TABLE-2
IMPEDANCE PARAMETERS OF MILD STEEL IN 1 M HCl SOLUTION WITH DIFFERENT CONCENTRATIONS OF INHIBITORS (2-APN AND ACN) AT 303 K

Inhibitors	Conc. (mM)	R_s (Ω cm^2)	R_p (Ω cm^2)	CPE_1		CPE_2		η (%)
				Y_0 ($\mu\Omega^{-1}$ s^n cm^{-2})	n_1	Y_0 ($\mu\Omega^{-1}$ s^n cm^{-2})	n_2	
Blank	0.00	0.82	14.5	364.0	0.80	–	0.00	–
2-APN	0.10	0.92	70.5	25.3	0.99	552.0	0.54	79.4
	0.25	0.87	92.0	27.7	0.99	599.1	0.52	84.2
	0.50	1.12	158.3	20.9	0.99	231.0	0.65	90.8
	1.00	1.08	227.6	13.7	0.99	233.5	0.62	93.6
	2.00	2.60	374.7	11.1	0.99	176.3	0.67	96.1
ACN	0.10	0.85	32.3	47.1	0.99	1493.0	0.60	55.1
	0.25	0.97	39.2	55.0	0.99	1115.0	0.68	63.0
	0.50	1.18	70.4	41.3	0.99	1160.0	0.40	79.5
	1.00	1.14	74.5	22.0	0.99	402.5	0.61	80.5
	2.00	1.05	99.2	22.6	0.99	405.7	0.60	85.4

increase in the thickness of electrical double layer by replacing water molecules or ions adsorbed originally on the surface by inhibitor molecules [27-29]. The EIS results show that the inhibition efficiency increases in the order of ACN < 2-APN.

Quantum chemical calculations: As the experimental work has been carried out in acidic medium, where inhibitor molecules get protonated, hence quantum chemical calculations were performed for both the neutral as well as protonated inhibitor molecules. The quantum chemical parameters like E_{HOMO} (the energy of the highest occupied molecular orbital), E_{LUMO} (the energy of the lowest unoccupied molecular orbital) and μ (dipole moment) for both the neutral as well as the protonated inhibitors are listed in Table-3. The ionization energy (I.E.) and electron affinity (E.A.) are calculated by the following equation [30-32]:

$$\text{Ionization energy (I.E.)} = - E_{HOMO} \quad (5)$$

$$\text{Electron affinity (E.A.)} = - E_{LUMO} \quad (6)$$

TABLE-3
THE QUANTUM CHEMICAL PARAMETERS OF THE NEUTRAL FORM OF THE INHIBITORS OBTAINED FROM DFT AT B3LYP/6-31++G (d.p) LEVEL

Quantum chemical parameters	2-APN		ACN	
	Neutral	Protonated	Neutral	Protonated
E_{HOMO} (e.V)	- 6.59	- 6.72	- 6.32	- 6.42
E_{LUMO} (e.V)	- 2.01	- 2.16	- 2.01	- 2.04
μ (D)	4.80	7.71	3.27	5.27

It is accepted that inhibitors are likely to be electron donor and the value of E_{HOMO} is associated with the electron donating ability of a molecule. Similarly, the value of E_{LUMO} is the measurements of electron accepting ability of the molecule from metallic iron surface [33-35]. Table-3 shows that E_{LUMO} value for both the inhibitors in neutral forms are same, while in protonated form E_{LUMO} for 2-APN is lower than ACN indicating higher electron accepting ability of 2-APN than that of ACN. The values of E_{HOMO} for the neutral as well as protonated molecules follow the order of ACN > 2-APN. Obviously, the sequence of E_{HOMO} is not in the order of experimental inhibition efficiency indicating complex nature of inhibition mechanism of the inhibitors. Literature reveals that the dipole moment of the inhibitor molecule is also an important parameter. However, literature reports are not consistent with the value of dipole moment; though, it is generally agreed that higher dipole moment favours higher adsorption and better inhibition of the inhibitor [36-39]. Dipole moment for both the neutral as well as protonated molecules follows the order: 2-APN > ACN, which is in good agreement with that of experimental inhibition efficiency. Thus there is good correlation between inhibition efficiency and electronic parameters like E_{HOMO} and dipole moment. It is worth noting that molecular electronic parameters are not secure parameters which could undoubtedly determine the inhibition ability of the inhibitor. As corrosion is a very complex process and various factors like pH, temperature, physical nature of the metal surface, *etc*. affect the inhibitive ability, while these factors are not considered into the quantum chemical calculations.

The optimized molecular structures, HOMO and LUMO molecular orbitals for the neutral 2-APN and ACN molecules are shown in Fig. 5. The frontier orbital electron density distribution is very useful in predicting preferable adsorption sites of the inhibitor molecules on the surface of the metal. It is observed that the electron density distribution in HOMO for 2-APN and ACN are similar and localized mainly in the pyridine ring of acetyl pyridine, C=N as well as C=O moiety in both the inhibitors, suggested that these are the probably important sites of the adsorption. In addition, electron distribution in LUMO is similar for both 2-APN and ACN and these are almost homogeneously distributed over whole molecular surface. It indicates that these molecules are also able to accept electrons from $4s^2$ orbital of the iron metal forming metal to inhibitor back bonding.

Adsorption isotherms: Potentiodynamic polarization measurements at 30 ºC in the presence of different concentration of the inhibitors are tested graphically by fitting to various isotherms like Langmuir, Frumkin and Temkin isotherms. The plot of C/θ *vs.* C gives straight line with linear correlation coefficient (R^2) close to unity for both the inhibitors (Fig. 6). It shows that the adsorption of 2-APN and ACN obey Langmuir adsorption isotherm (eqn. 7).

$$\frac{C}{\theta} = \frac{1}{K_{ads}} + C \quad (7)$$

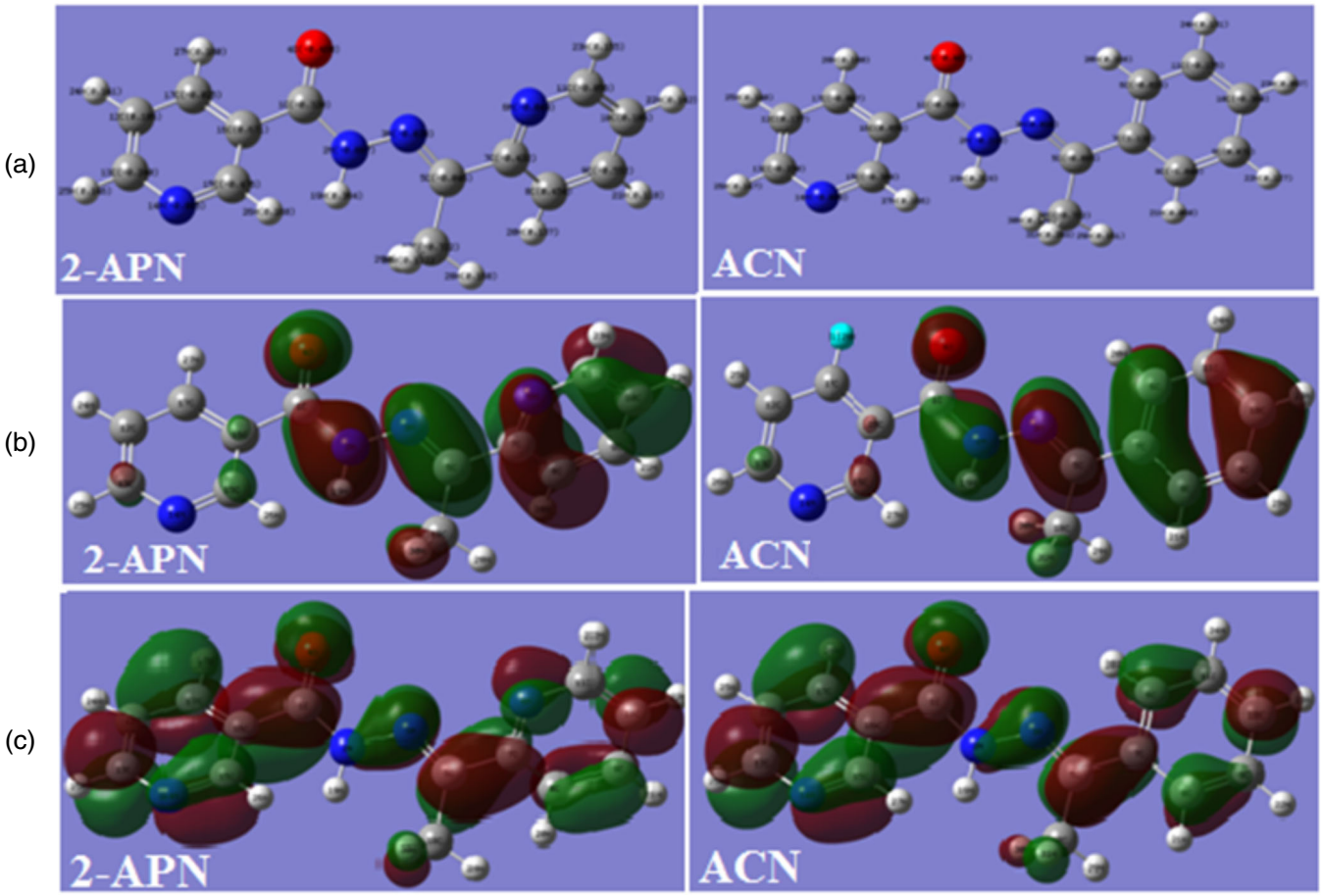

Fig. 5. (a) Optimized molecular structure (b) HOMO and (c) LUMO diagrams for the neutral 2-APN and ACN by DFT method at B3LYP/6-31++G (d,p) basis set

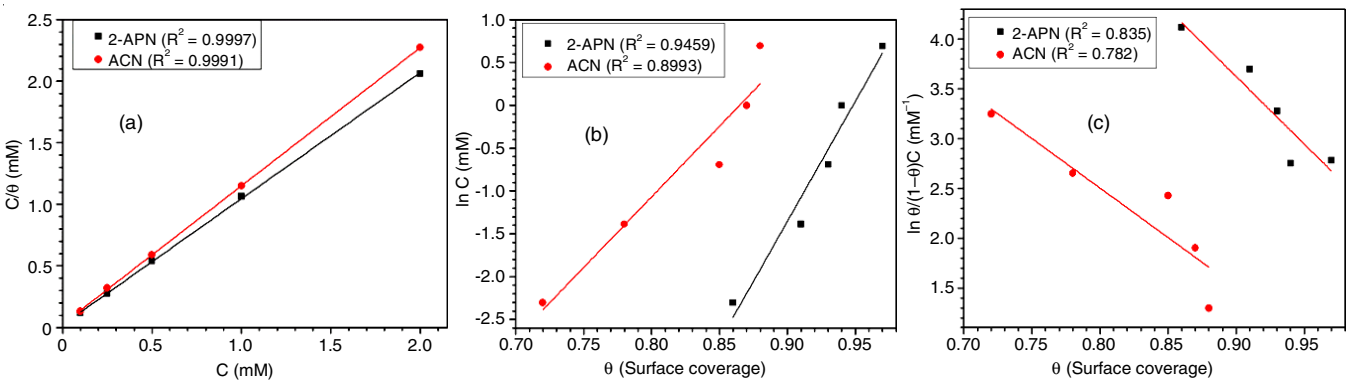

Fig. 6. Adsorption isotherms for mild steel in 1 M HCl with 2-APN and ACN at 30 °C: (a) Langmuir, (b) Temkin and (c) Frumkin

where C is the inhibitor concentration, θ is the degree of surface coverage and K_{ads} is the equilibrium adsorption constant. The K_{ads} value can be determined from the intercepts of the straight lines. The relationship of K_{ads} with standard free energy of adsorption (ΔG°_{ads}) can be represented as [40,41]:

$$K_{ads} = \frac{1}{55.5}\exp\left(-\frac{\Delta G^{\circ}_{ads}}{RT}\right) \quad (8)$$

where 55.5 is the molar concentration of water in the solution expressed in M (mol L^{-1}), R is the gas constant (8.314 J K^{-1} mol^{-1}) and T is the absolute temperature (K). The calculated values of K_{ads} for 2-APN and ACN are 4.7×10^4 M^{-1} and 3.7×10^4 M^{-1}, respectively indicating higher adsorption tendency of both the inhibitors on the mild steel surface. It is believed that the -ΔG° values of 20 kJ mol^{-1} or less associated with physisorption *i.e.*, electrostatic attraction between charged inhibitor molecules and charged metal surface, while those of 40 kJ mol^{-1} or more indicates chemisorption [42-45]. The value of -ΔG° for 2-APN and ACN are 36.68 kJ mol^{-1} and 37.00 kJ mol^{-1}, respectively. It indicates that the adsorption of inhibitors on the mild steel surface is spontaneous and involve both physisorption and chemisorption mode of mechanism.

Activation energy (E_a): The activation energy (E_a) of the corrosion process has been calculated by weight loss measurements in the absence and presence of the inhibitors at 2 mM in the temperature range of 303-323 K. The relationship between the activation energy and corrosion rate for the corrosion process can be given by the Arrhenius equation as:

$$\log C_R = \log A - \frac{E_a}{2.303RT} \quad (9)$$

where C_R is the corrosion rate, A is the Arrhenius constant, E_a is the activation energy, T is the absolute temperature and R is the gas constant. The value of activation energy for the mild steel in the presence and absence of inhibitors can be calculated from the slopes of the Arrhenius plots of log C_R *vs.* 1/T as shown in Fig. 7. The E_a values for the corrosion of mild steel in 1 M HCl in the presence and absence of 2 mM of the inhibitors suggested that 2-APN (39.11 kJ mol^{-1}) and ACN (47.08 kJ mol^{-1}) are slightly lower than that of uninhibited solution (47.64 kJ mol^{-1}). The decrease in activation energy in the presence of inhibitors suggest chemisorption. Moreover, it is very difficult to come on conclusion about the mechanism of adsorption just only on the basis of the value of activation energy due to competitive adsorption with water molecules, whose removal from the surface also requires some activation energy. Therefore, it may be concluded that the adsorption of inhibitors from 1 M HCl solution involves both the physical and chemical processes simultaneously [46-49].

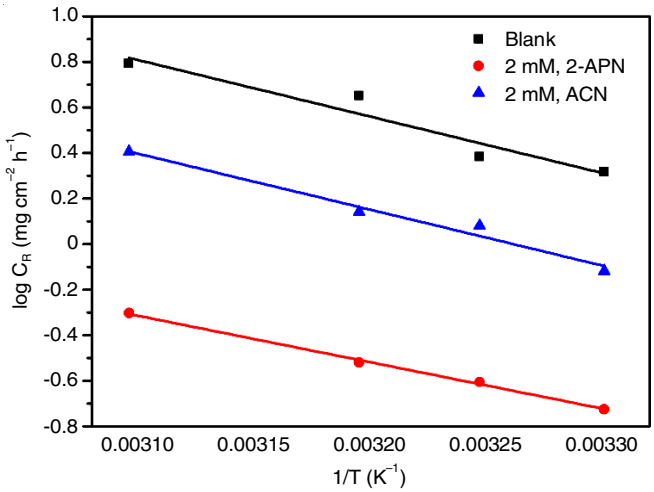

Fig. 7. Arrhenius plots of log C_R *vs.* 1/T for mild steel in 1 M HCl in the presence and absence of 2 mM of the inhibitors

Conclusion

Two nicotinic hydrazone (Schiff bases) were synthesized namely 2-acetyl pyridine nicotinic hydrazone (2-APN) and acetophenone nicotinic hydrazone (ACN) and investigated as corrosion inhibitors for mild steel in 1 M HCl. The inhibition efficiency of both the inhibitors increases with increase in concentration. The maximum inhibition efficiency of 2-APN and ACN at 2 mM was found to be 96.5% and 87.7%, respectively. Potentiodynamic polarization measurements suggest that they can be classified as mixed type inhibitors. Electrochemical impedance spectroscopy (EIS) measurements depicted an increase of polarization resistance (R_p) and decrease in the value of CPE in the presence of 2-APN and ACN. The adsorption of 2-APN and ACN obey Langmuir adsorption isotherm only. The values of ΔG^o for 2-APN and ACN were -36.68 kJ mol^{-1} and -37.00 kJ mol^{-1}, respectively. The quantum chemical parameters calculated by DFT method like E_{LUMO} in the gaseous as well as aqueous phase follow the order: 2-APN < ACN; which is in good agreement with the experimental results. The higher inhibition performance shown by 2-APN compared to ACN may be attributed to the presence of higher number of pyridine rings/moieties in the structure of 2-APN, which has higher complex formation ability.

ACKNOWLEDGEMENTS

The authors gratefully acknowledge Indian Institute of Technology (Indian School of Mines), Dhanbad, India for providing experimental facilities to carry out this work.

CONFLICT OF INTEREST

The authors declare that there is no conflict of interests regarding the publication of this article.

REFERENCES

1. F. Bentiss, M. Lebrini, M. Traisnel and M. Lagrenée, *J. Appl. Electrochem.*, **39**, 1399 (2009); https://doi.org/10.1007/s10800-009-9810-9
2. B. El-Mehdi, B. Mernari, M. Traisnel, F. Bentiss and M. Lagrenée, *Mater. Chem. Phys.*, **77**, 489 (2003); https://doi.org/10.1016/S0254-0584(02)00085-8
3. K.M. Govindaraju, D. Gopi and L. Kavitha, *J. Appl. Electrochem.*, **39**, 2345 (2009); https://doi.org/10.1007/s10800-009-9920-4
4. M. Behpour, S.M. Ghoreishi, A. Gandomi-Niasar, N. Soltani and M. Salavati-Niasari, *J. Mater. Sci.*, **44**, 2444 (2009); https://doi.org/10.1007/s10853-009-3309-y
5. E.S. Ferreira, C. Giacomelli, F.C. Giacomelli and A. Spinelli, *Mater. Chem. Phys.*, **83**, 129 (2004); https://doi.org/10.1016/j.matchemphys.2003.09.020
6. C.M. Goulart, A. Esteves-Souza, C.A. Martinez-Huitle, C.J.F. Rodrigues, M.A.M. Maciel and A. Echevarria, *Corros. Sci.*, **67**, 281 (2013); https://doi.org/10.1016/j.corsci.2012.10.029
7. E.E. Ebenso and I.B. Obot, *Int. J. Electrochem. Sci.*, **5**, 2012 (2010).
8. S.K. Shukla and M.A. Quraishi, *Corros. Sci.*, **51**, 1007 (2009); https://doi.org/10.1016/j.corsci.2009.02.024
9. B. Xu, W. Yang, Y. Liu, X. Yin, W. Gong and Y. Chen, *Corros. Sci.*, **78**, 260 (2014); https://doi.org/10.1016/j.corsci.2013.10.007
10. B.D. Mert, M. Erman Mert, G. Kardas and B. Yazici, *Corros. Sci.*, **53**, 4265 (2011); https://doi.org/10.1016/j.corsci.2011.08.038
11. M.R. Maurya, S. Agarwal, M. Abid, A. Azam, C. Bader, M. Ebel, D. Rehder, *Dalton. Trans.*, **21**, 937 (2006); https://doi.org/10.1039/B512326G
12. D.K. Singh, S. Kumar, G. Udayabhanu and R.P. John, *J. Mol. Liq.*, **216**, 738 (2016); https://doi.org/10.1016/j.molliq.2016.02.012
13. D.K. Singh, E.E. Ebenso, M.K. Singh, D. Behera, G. Udayabhanu and R.P. John, *J. Mol. Liq.*, **250**, 88 (2018); https://doi.org/10.1016/j.molliq.2017.11.132
14. R. Yildiz, *Corros. Sci.*, **90**, 544 (2015); https://doi.org/10.1016/j.corsci.2014.10.047
15. Q.B. Zhang and Y.X. Hua, *Electrochim. Acta*, **54**, 1881 (2009); https://doi.org/10.1016/j.electacta.2008.10.025

16. R. Solmaz, G. Kardas, M. Culha, B. Yazici and M. Erbil, *Electrochim. Acta*, **53**, 5941 (20080); https://doi.org/10.1016/j.electacta.2008.03.055
17. F. Bentiss, M. Lagrenee, M. Traisnel and J.C. Hornez, *Corros. Sci.*, **41**, 789 (1999); https://doi.org/10.1016/S0010-938X(98)00153-X
18. R. Solmaz, G. Kardas, B. Yazici and M. Erbil, *Colloids Surf. A Physicochem. Eng. Asp.*, **312**, 7 (2008); https://doi.org/10.1016/j.colsurfa.2007.06.035
19. X. Wang, H. Yang and F. Wang, *Corros. Sci.*, **53**, 113 (2011); https://doi.org/10.1016/j.corsci.2010.09.029
20. S.K. Saha, A. Dutta, P. Ghosh, D. Sukul and P. Banerjee, *Phys. Chem. Chem. Phys.*, **18**, 17898 (2016); https://doi.org/10.1039/C6CP01993E
21. A. Doner, R. Solmaz, M. Ozcan and G. Kardas, *Corros. Sci.*, **53**, 2902 (2011); https://doi.org/10.1016/j.corsci.2011.05.027
22. M. Erbil, *Chim. Acta Turc.*, **1**, 59 (1988).
23. G. Avci, *Mater. Chem. Phys.*, **112**, 234 (2008); https://doi.org/10.1016/j.matchemphys.2008.05.036
24. M. Ozcan, I. Dehri and M. Erbil, *Appl. Surf. Sci.*, **236**, 155 (2004); https://doi.org/10.1016/j.apsusc.2004.04.017
25. T. Pajkossy, *J. Electroanal. Chem.*, **364**, 111 (1994); https://doi.org/10.1016/0022-0728(93)02949-I
26. F. Mansfeld, Z. Sun, C.H. Hsu and A. Nagiub, *Corros. Sci.*, **43**, 341 (2001); https://doi.org/10.1016/S0010-938X(00)00064-0
27. A.O. Yüce and G. Kardaº, *Corros. Sci.*, **58**, 86 (2012); https://doi.org/10.1016/j.corsci.2012.01.013
28. A.K. Singh and M.A. Quraishi, *Corros. Sci.*, **51**, 2752 (2009); https://doi.org/10.1016/j.corsci.2009.07.011
29. M. Mahdavian and S. Ashhari, *Electrochim. Acta*, **55**, 1720 (2010); https://doi.org/10.1016/j.electacta.2009.10.055
30. K.F. Khaled, *Electrochim. Acta*, **55**, 6523 (2010); https://doi.org/10.1016/j.electacta.2010.06.027
31. Z. El Adnani, M. Mcharfi, M. Sfaira, M. Benzakour, A.T. Benjelloun and M. Ebn Touhami, *Corros. Sci.*, **68**, 223 (2013); https://doi.org/10.1016/j.corsci.2012.11.020
32. I.B. Obot and N.O. Obi-Egbedi, *Corros. Sci.*, **52**, 657 (2010); https://doi.org/10.1016/j.corsci.2009.10.017
33. I. Ahamad, R. Prasad and M.A. Quraishi, *Corros. Sci.*, **52**, 933 (2010); https://doi.org/10.1016/j.corsci.2009.11.016
34. G. Gao and C. Liang, *Electrochim. Acta*, **52**, 4554 (2007); https://doi.org/10.1016/j.electacta.2006.12.058
35. S.E. Nataraja, T.V. Venkatesha, H.C. Tandon and B.S. Shylesha, *Corros. Sci.*, **53**, 4109 (2011); https://doi.org/10.1016/j.corsci.2011.08.019
36. K.F. Khaled, *Corros. Sci.*, **52**, 2905 (2010); https://doi.org/10.1016/j.corsci.2010.05.001
37. I. Fleming, Frontier Orbitals and Organic Chemical Reactions, John Wiley and Sons: New York (1976).
38. T. Chakraborty, K. Gazi and D.C. Ghosh, *Mol. Phys.*, **108**, 2081 (2010); https://doi.org/10.1080/00268976.2010.505208
39. L. Li, Q. Qu, W. Bai, F.C. Yang, Y.J. Chen, S.W. Zhang and Z.T. Ding, *Corros. Sci.*, **59**, 249 (2012); https://doi.org/10.1016/j.corsci.2012.03.008
40. X. Ma, X. Jiang, S. Xia, M. Shan, X. Li, L. Yu and Q. Tang, *Appl. Surf. Sci.*, **371**, 248 (2016); https://doi.org/10.1016/j.apsusc.2016.02.212
41. M.J. Bahrami, M.A. Hosseini and P. Pilvar, *Corros. Sci.*, **52**, 2793 (2010); https://doi.org/10.1016/j.corsci.2010.04.024
42. S.K. Shukla and M.A. Quraishi, *Corros. Sci.*, **51**, 1990 (2009); https://doi.org/10.1016/j.corsci.2009.05.020
43. E. Machnikova, K.H. Whitmire and N. Hackerman, *Electrochim. Acta*, **53**, 6024 (2008); https://doi.org/10.1016/j.electacta.2008.03.021
44. I. Ahamad and M.A. Quraishi, *Corros. Sci.*, **51**, 2006 (2009); https://doi.org/10.1016/j.corsci.2009.05.026
45. B.G. Ateya, B.E. El-Anadouli and F.M.A. El-Nizamy, *Corros. Sci.*, **24**, 497 (1984); https://doi.org/10.1016/0010-938X(84)90032-5
46. L. Vracar and D.M. Drazic, *Corros. Sci.*, **44**, 1669 (2002); https://doi.org/10.1016/S0010-938X(01)00166-4
47. Y. Tang, F. Zhang, S. Hu, Z. Cao, Z. Wu and W. Jing, *Corros. Sci.*, **74**, 271 (2013); https://doi.org/10.1016/j.corsci.2013.04.053
48. F.M. Donahue and K. Nobe, *J. Electrochem. Soc.*, **112**, 886 (1965); https://doi.org/10.1149/1.2423723
49. E. Khamis, F. Bellucci, R.M. Latanision and E.S.H. El-Ashry, *Corrosion*, **47**, 677 (1991); https://doi.org/10.5006/1.3585307